Femtosecond spectroscopic study of carminic acid–DNA interactions

R. Comanici, B. Gabel, T. Gustavsson, D. Markovitsi, C. Cornaggia, S. Pommeret, C. Rusu, C. Kryschi

Femtosecond spectroscopic study of carminic acid-DNA interactions

Radu Comanici[a], Bianca Gabel[a], Thomas Gustavsson[b], Dimitra Markovitsi[b], Christian Cornaggia[c], Stanislas Pommeret[d], Catalin Rusu[a], and Carola Kryschi[a,*]

[a] Department of Physical Chemistry I, Friedrich-Alexander University, D-91058 Erlangen, Germany

[b] Laboratoire Francis Perrin, CEA/DSM/DRECAM/SPAM - CNRS URA 2453
CEA Saclay, 91191 Gif-sur-Yvette, France

[c] Laboratoire Francis Perrin, CEA/DSM/DRECAM/SPAM - CNRS URA 2453
CEA Saclay, 91191 Gif-sur-Yvette, France

[d] Laboratoire Claude Fréjacques, CEA/DSM/DRECAM/SCM - CNRS URA 311
CEA Saclay, 91191 Gif-sur-Yvette, France

Abstract

Photo-excited carminic acid and carminic acid-DNA complexes in a buffer solution at pH= 7 have been examined using a variety of spectroscopy techniques, that are in particular, the femtosecond resolved fluorescence up-conversion and transient absorption spectroscopy. The observation of dual fluorescence emission, one peaks at 470 nm and the other at 570 nm, indicates to an excited-state (S_1) intramolecular proton transfer (ESIPT). A detailed analysis of the transient absorption measurements of an aqueous carminic-acid solution at pH= 7 yielded four lifetimes for the excited state (S_1): 8 ps, 15 ps, 33 ps and 46 ps. On the other hand, only two lifetimes, 34 ps and 47 ps, were observed by fluorescence up-conversion spectroscopy because of the detection limitation to the long wavelength edge of the carminic-acid spectrum. The four S_1 lifetimes were ascribed to the coexistence of respectively two tautomer (normal and tautomer) forms of carminic acid, in the nondissociated state (CAH) and in the deprotonated state (CA^-). The fluorescence up-conversion measurements of

carminic acid-DNA complexes exhibited a prolongation of the fluorescence lifetimes. This effect was accepted as evidence for the formation of intercalation complexes between the carminic acid and the DNA. The intercalative binding of the carminic acid to DNA was confirmed by the fluorescence titration experiments resulting to a binding constant of 2×10^5 M^{-1} that is typical for anthracycline-DNA complexes.

*To whom correspondence should be addressed:

Department of Physical Chemistry I

Friedrich-Alexander University

Egerlandstr. 3, D-91058 Erlangen, Germany

1. Introduction

Antitumor and antibiotics anthracyclines have been extensively studied for decades in an effort to optimize their therapeutic function for the treatment of various human cancers. These compounds are believed to develop their cytotoxic effect by penetrating into the tumor cell nucleus and interacting there with DNA [1-4]. The formation of drug-DNA complexes is determined by the structural features of the anthracyclines composed of a dihydroxy-anthraquinone chromophore with one or two gycosyl side chains. The carboxy and hydroxy groups provide for the water solubility, whereas binding to DNA occurs via inserting of the glycosyl groups into the grooves of DNA and by subsequent intercalating of the chromophore between the CG base pairs of DNA. The intercalation process is followed by conformational relaxation of the anthracycline-DNA complex [3,4]. Formation of intercalation complexes has been observed to inhibit the DNA replication and the RNA transcription that blocks the gene expression [3]. Irradiation with light enhances the cytotoxicity of anthracyclines (*e.g.* daunomycin) by several orders of magnitudes [5-8]. This photoactivation effect is understood to originate from an ultrafast electron transfer reaction from a G base of DNA to the intercalated chromophore, which is associated with the oxidation of the G base and the reduction of the intercalated dihydroxyanthraquinone [7,8]. This hypothesis is based on femtosecond spectroscopy studies of daunomycin-DNA and adriamycin-DNA complexes, yielding a decrease of the S_1 state lifetime of the drug by three orders of magnitude when DNA is present [7]. The lifetime of the daunomycin-DNA complex with τ= 290 fs was ascribed to photo-induced electron transfer occurring from the G base to the 1,4-dihydroxyanthraquinone chromophore. On the other hand, other radiationless decay processes such as intersystem crossing, internal conversion and excited-state intramolecular proton transfer (ESIPT) may also be enhanced by the conformational changes and solvatochromic effects that daunomycin experiences in the hydrophobic environment of the DNA base pair stackings. Despite extensive research activities on the examination of photo-activated

anthracycline-DNA complexes [7-11], to this date there exists no unambiguous evidence for photo-induced oxidation of the DNA and moreover, the excited-state relaxation dynamics as well as the structural mechanism at the molecular level are more hypothetical than really understood. In particular, tautomerization reactions of hydroxyanthraquinone-DNA complexes are completely ignored.

In this contribution we present a femtosecond-resolved transient absorption spectroscopy and fluorescence up-conversion spectroscopy study of carminic acid-DNA complexes. We have focused onto carminic acid (7-α-D-glycopyranosyl)-9,10,dihydro-3,5,6,8-tetrahydroxy-1-methyl-9,10-dioxo-2-anthracenecarboxylic acid), since this natural dye consists of a tetrahydoxy-anthraquinone chromophore with a pendant glycosyl moiety and thus constitutes the essential structural features of the anthracyclines. The main impetus for us is to understand the complex mechanism and dynamics of the excited-state relaxation of carminic acid in the presence of DNA. Carminic acid as a carboxylic acid is expected to dissociate in water, so that two forms should coexist at pH=7, the fully protonated acid (CAH) and the deprotonated anion (CA^-) (see Scheme 1). The anthraquinone chromophore contains four hydroxy groups with two of them posititioned in direct neighborhood of one central oxo group, respectively. These keto-enol pair structures enable two single proton transfers and one double proton transfer and therewith suggest the coexistence of the normal form (CAH) and three tautomers (T1, T2, T3) (see Scheme 2).

Although the uv/vis absorption spectra and the fluorescence spectra of carminic acid and their dependence on the pH value had been investigated in detail [12-14], no contribution of tautomerization reactions, that may occur in the ground state (S_0) as well as in the excited state (S_1), to the spectroscopic properties were taken into account. This is really surprising, since excited-state intramolecular proton transfer (ESIPT) has been shown to accelerate the rate of internal conversion by reducing the energy gap between the S_0 and S_1 state [14]. In

order to get a better insight into the ESIPT kinetics of carminic acid and its sensitivity to the microenvironment of the DNA base stacks, we have performed ZINDO/S calculations of the electronic spectra of the four carminic acid tautomers in both its non dissociated and dissociated forms. In addition, we have studied the binding of carminic acid to DNA performing fluorescence titration experiments.

2. Experimental

Chemicals. Carminic acid was purchased from Aldrich (99% purity) and was used without further purification. Salmon sperm DNA was obtained from Sigma. The DNA concentrations were determined by uv/vis absorption spectroscopy measurements at 260 nm using the extinction coefficient ε= 6600 (M nucleotide)$^{-1}$ cm^{-1}. Ultrapure water was obtained from a MilliPore system. The buffer designated as BPES [10] consists of MilliPore water with 6 mM Na_2HPO_4, 2 mM NaH_2PO_4, 1 mM Na_2EDTA, and 185 mM NaCl and has a pH= 7.0. Uv/vis absorption spectroscopy and fluorescence spectroscopy measurements of carminic acid in BPES, MilliPore water or dimethylsulfoxide (DMSO) (Merck, pro analysi) were performed at carminic acid concentrations between 5 µM and 10 µM, if nothing else is reported. Sample solutions (carminic acid in BPES) used for the fs resolved spectroscopic investigations were prepared to have an optical density of about 0.5 at 400 nm for an optical path of 0.4 mm or 2 mm. For the determination of the pK_a value of carminic acid in BPES we have titrated carminic acid in MilliPore water at a concentration of 5 µM or 1 mM with an aqueous 5µM NaOH solution *(e.g.* 1 mM NaOH). The pH value was potentiometrically measured using a pH meter (pH 522, WTW) equipped with a glass electrode (pH Electrode BlueLine 23pH, Schott).

Uv/vis absorption and fluorescence spectroscopy experiments. Uv/vis absorption spectra of carminic acid in BPES, in MilliPore water or in DMSO were recorded on a Perkin-Elmer

Lambda2 spectrometer. The fluorescence spectra were taken with a Jobin-Yvon FluoroMax-3 spectrofluorometer in the magic-angle polarization configuration. All the stationary spectroscopy experiments were performed at room temperature employing quartz cuvettes with an optical path length of 10 mm and for carminic acid concentrations between 5 and 10 μM. The fluorescence quantum yield Φ of carminic acid in MilliPore water was determined with reference to rhodamine 6G in ethanol (Φ_0= 95 % [15]) using the relationship:

$$\Phi = \Phi_0 \frac{S(1-10^{-A_0}) \cdot n^2}{S_0(1-10^{-A}) \cdot {n_0}^2}$$

where S and S_0 are the integral intensities of the fluorescence spectra measured in the magic-angle polarization configuration in the range of 500 - 800 nm, A and A_0 are the absorbances at the excitation wavelength of 480 nm of carminic acid and rhodamine 6G, respectively, n denotes the refractive index of water and n_0 that of ethanol.

Fluorescence Titration Experiments. For the fluorescence titration experiments an excitation wavelength of λ_{exc} = 320 nm with a slit width of 10 nm was typically used, and the spectrum was recorded from 360 nm to 800 nm with a slit width of 10 nm. The relative fluorescence intensities were determined by integrating over the whole spectrum.

Femtosecond transient absorption spectroscopy and up-conversion fluorescence spectroscopy. The setup used for the femtosecond transient absorption spectroscopy [16] is based on a Ti:sapphire laser system that consists of a mode-locked oscillator (Coherent, Mira) pumped by an argon ion laser (Coherent, Innova 310) and a Ti:Sapphire regenerative amplifier (Alpha 1000 US, BM Industries). This femtosecond laser system produces 40 fs output pulses at 800 nm with a repetition rate of 1 kHz and energies of about 700 μJ. The pump pulses at 400 nm were obtained by frequency doubling the output pulses in a 0.2 mm BBO crystal, whereas white-light continuum pulses between 400 and 800 nm were generated

by focussing a small fraction of the fundamental pulses into a thin rotating fused silica disc. By applying the pump pulses at 400 nm to the sample solution, carminic acid was non-resonantly excited into the S_1 state, while the excited-state decay dynamics were probed with the temporally delayed white-light continuum pulses.

Transient absorption spectra were obtained by determining the differential absorption in the sample versus the delay time τ between the pump and the white-light continuum pulses. To compensate for eventual intensity fluctuations, the white-light continuum was split into two parts, one overlapping with the pump beam in the sample and thus serving as probe pulse and whereas the other one, non-overlapping with the pump beam, was used as a reference. After passage through the sample, both, probe and reference beams were dispersed in a spectrograph (Spex 270M) and detected using a 1024x512 pixels CCD camera (Princeton Instruments). The readout rate of the camera was 30 Hz achieved by a chopper that modulates both beams.

The transmitted white–light intensity of the probe (T_{sample}) and the reference (T_{ref}) beams were simultaneously measured on the CCD for delay times $\tau \geq 0$ ps. The delay time was varied between 0 and 200 ps by 30 fs steps. The differential absorption is defined by the equation

$$absorption = \log\left[\frac{T_{sample}(\tau)}{T_{ref}(\tau)}\right] - \log\left[\frac{T_{sample}(\tau<0)}{T_{ref}(\tau<0)}\right].$$

In this equation, $T_{ref}(\tau)$ accounts for the transmission of the reference signal that was recorded simultaneously with the probe signal in order to compensate for any intensity fluctuations. By definition, the transient absorption is negative and the bleaching of the ground-state population density is positive. The sample solutions were pumped through a flow cell with a thickness of 0.4 mm or 2 mm. The 0.4 mm-thick flow cell was used for carminic acid concentrations between 1 and 6×10^{-4} M, whereas sample solutions at a concentration above

1×10^{-3} M were investigated in a 2 mm cell. The FWHM of the instrument response function is about 60 fs in the white-light continuum spectral range of 400 – 800 nm.

The fs-resolved fluorescence up-conversion experiments were performed using a setup that has been already described in detail elsewhere [17]. A fs laser system, consisting of a Ti:sapphire laser (Coherent MIRA 900), pumped by a 10 W cw solid state laser (Coherent VERDI V10), produces 125 fs pulses at 800 nm with a repetition rate of 76 MHz and a 1.8 W average output power. The second harmonic (SH) is generated in a 0.5 mm thick BBO crystal and is separated from the fundamental beam by a dichroic splitter. The SH is used as pump pulse for excitation of the fluorescence of the sample, whereas the fundamental pulse serves as gating pulse for the sum frequency ("up conversion") generation. The fluorescence light is focused into the up conversion crystal, and the up converted light is spectrally analyzed using a 220 mm focal length double grating monochromator (SPEX 1680). The detection and amplification of the dispersed up conversion light is achieved by using a photomultiplier (Hamamatsu R1527P) in combination with a photon counter (Stanford SR400). The fluorescence up conversion experiments were performed at 0° and 90° angle between the polarization axes of excitation and detection. The cross correlation trace between the laser fundamental (800 nm) and the SH (400 nm) gives a FWHM value of 175 fs for the apparatus function.

Fluorescence up conversion spectra were corrected first by subtracting the background from the fluorescence up conversion spectra. The background was recorded by positioning the delay at "negative" time, so that the gating pulse arrives to the up conversion crystal well before the fluorescence signal. The current spectral correction curve, $R(\lambda)$, was determined experimentally by comparing the normalized fluorescence up conversion spectrum at long times (100 ps: $I^{100ps}(\lambda)$) with the normalized steady state spectrum, $I^{SS}(\lambda)$ recorded for the

same sample solution, so that the relationship $R(\lambda)=I^{SS}(\lambda)/I^{100ps}(\lambda)$ was obtained. All fluorescence up conversion spectra were subsequently multiplied with $R(\lambda)$.

Computations. Semiempirical quantum chemical computations of the molecular geometries, orbitals and electronic energy states of the four carminic acid tautomers in the fully protonated state (CaH) as well as in the singly deprotonated state (CA^-) were performed using the HYPERCHEM (release 7.1) package program. The geometry optimizations of all structures were achieved employing the ZINDO/S self-consistent fields molecular orbital (SCF MO) method at the restricted Hartree-Fock (RHF) level [18]. For the optimizations we have applied the steepest-descent method in combination with the consecutively performed conjugate gradient methods, Fletcher-Rieves and Polak-Ribiere (convergence limit of 4.18×10^{-4} kJ/mol and RMS gradient of 4.18×10^{7} kJ/m mol). RHF open-shell and closed-shell calculations of the electronic energy states and of the electronic transitions were performed for single configuration interaction (CI) involving 160 total orbitals.

3. Results and discussion

A. Stationary spectroscopy experiments and semiempirical computations

Carminic acid possesses a carboxylic acid function and is expected to dissociate in water (*see* Scheme 1). Upon performing titration measurements of carminic acid in Millipore water with NaOH against a pH meter we have determined a value of pK_a= 5.55. This implies that the dissociation equilibrium at pH= 7 is adjusted to nearly equal concentrations of non dissociated carminic acid (CAH) and of its deprotonated form (CA^-). Photo-exciting carminic acid in BPES with 340 nm light generates two fluorescence emissions, one peaks at 15100 cm^{-1} (570 nm: orange emission) and the other at 22700 cm^{-1} (470 nm: blue emission) (*see* Fig.1, left panel). The intensity of the orange fluorescence is half of the blue fluorescence intensity. The observation of the dual fluorescence is taken as strong indication to an excited state

intramolecular proton transfer (ESIPT) [19-23]. Mostly, the excited-state (S_1) tautomer accessed by ESIPT has an energy comparable to or slightly less than that of the normal form, while the ground state (S_0) of the tautomer is of considerably higher energy. As a consequence, the fluorescence of the tautomer appears spectrally red shifted with respect of that of the normal form. That is why we ascribe the blue fluorescence to the normal form, whereas we expect the tautomer to emit the orange fluorescence. In contrast, carminic acid that was dissolved in the aprotic solvent DMSO and was analogously photo-excited at 340 nm, exhibited the orange fluorescence only (*see* Fig. 1, right panel). The lack of the blue fluorescence implies that the ESIPT occurs in this aprotic solvent with a rather high probability. This is explained by the fact that DMSO does not form external H bondings, which stabilize the normal form of carminic acid against the ESIPT as it occurs in water. Another stabilization effect may arise from efficient interactions of DNA with carminic acid. Photo-excited BPES sample solutions, containing the same concentrations of carminic acid and DNA with 5 µM, were observed to emit the blue fluorescence with a significantly higher intensity than that of the orange fluorescence (*see* Fig.2). For carminic acid in BPES the ratio of orange fluorescence intensity to blue fluorescence intensity amounts to 2:1, whereas that one in the presence of DNA is 0.8:1. The increase of the blue fluorescence intensity at the expense of the orange fluorescence intensity does not only indicate to strong interactions between DNA and carminic acid, but also manifests that the intercalated carminic acids experiences a significant structural stabilization due to its rigid environment in the base pair stacks of DNA.

In order to obtain information of the dissociation equilibrium in the S_0 state, we have recorded the uv/vis absorption spectra of carminic acid in BPES (*see* Fig.3, left panel) and carminic acid in DMSO (*see* Fig.3, right panel). The band structure of both spectra (thin solid line) was analyzed by calculating them as a superposition of four Gaussian functions (dashed line). As expected the peak areas and the central positions of the four calculated peaks in the BPES

spectrum are different from those in the DMSO spectrum. The large red shifts of the peak positions in the carminic acid-BPES spectrum in comparison with that of DMSO are explained by the more efficient solvation that carminic acid experiences in water, since the water molecules form strong H bondings to the oxo and hydroxy groups of carminic acid. On the other hand, the peak areas are determined by the concentration of the respective species and their extinction coefficients (*i.e.* oscillatory strength). However, the appearance of these four peaks in the absorption spectrum indicates to the coexistence of four different geometric states of carminic acid in the S_0 state. Two of them are ascribed to non dissociated carminic acid and its deprotonated anion. The non dissociated acid as well as its deprotonated anion may undergo a tautomerization reaction in the ground state, and thus both may occur in a equilibrium distribution as the normal form and as one tautomer. These four species may also be formed in DMSO, since this solvent naturally contains water up to 2 vol %. In terms of this rationale the spectrum of carminic acid in BPES was analyzed as follows: the relatively large peaks at 22230 cm^{-1} and 19760 cm^{-1} were assigned to the normal and tautomer form of the nondissociated carminic acid (CAH and CAH T3, *see* Scheme 2), respectively, whereas the small peak at 19060 cm^{-1} and the very large one at 17890 cm^{-1} represent the lowest-energy absorption transitions of the deprotonated CA^- and its tautomer CA^- T3 (*see* Scheme 2). In the case of carminic acid in DMSO as containing water at ca. 2 vol % the two small peaks (18560 cm^{-1} and 19710 cm^{-1}) at the low-energy edge of the absorption spectrum were analogously ascribed to the absorption transitions of CA^-T3 and CA^-, respectively. The very large peak at 20340 cm^{-1} displays the absorption of CAH T3 and the smaller one at 22544 cm^{-1} that of CAH.

Complementary information about the different geometric states of carminic acid in BPES were obtained upon performing semiempirical ZINDO/S computations on respectively four tautomers of the non dissociated carminic acid and its deprotonated anion in vacuo. We have calculated the optimized geometries, electronic states and electronic transitions of all the eight

carminic acid structures. The results are summarized in Table 1. The non dissociated normal form of carminic acid (CAH) has the lowest absolute energy, E_{abs}= -8041.5 eV and the largest S_0-S_1 difference (22716 cm^{-1}) with a rather large oscillatory strength of f= 0.269, which supports our assignment of the highest-energy peaks in the absorption spectra. The similarly low absolute energy of the tautomer CAH T3 (E_{abs}= -8041.3 eV), its largely red-shifted absorption band (18900 cm^{-1}) and the still higher oscillatory strength of f= 0.393 also coincide nicely with the spectroscopy data and moreover, indicates to a S_0-state tautomerization equilibrium between CAH and CAH T3. Since the solvent shift in a polar medium such as water is expected to significantly differ for neutral and ionic species, the calculated absolute energy values of CA^- and CA^- T3, with E_{abs}= -8014.2 eV and E_{abs}= -8014.4 eV, respectively, cannot be correlated with those of non dissociated carminic acid. Nevertheless, the nearly equal absolute energy values of CA^- and CA^- T3 also suggest their coexistence in the ground state. The difference in their oscillatory strengths matches perfectly to the observation of a relatively small absorption peak of CA^- in comparison with the four times larger one of CA^- T3 (*see* Fig.3, left panel).

The absorption spectra and semiempirical computations support the hypothesis that the tautomers CAH T3 and CA^-T3 may be formed in the S_0 state. This has been confirmed by detecting the fluorescence of the tautomers subsequently to selective excitation at 480 nm. Fig. 4 depicts the fluorescence spectra recorded from a BPES solution (left panel) and from a DMSO solution (right panel). The Gaussian fit of the BPES spectrum yielded three peaks positioned at 16487 cm^{-1}, 14906 cm^{-1} and 14277 cm^{-1}. The 16487 cm^{-1} peak was assigned to the fluorescence of CAH T3, whereas the peaks at 14906 cm^{-1} and 14277 cm^{-1} display the fluorescence spectrum (electronic and vibronic transition) of CA^- T3. The analysis of the DMSO spectrum resulted into two peaks (at 17440 cm^{-1} and 16487 cm^{-1}) only, which were ascribed to fluorescence transitions of CAH T3.

The fluorescence quantum yield of the carminic acid tautomers dissolved in Millipore water was determined as a value of 2.7 %. This rather low fluorescence quantum yield suggests that the deactivation of the S_1 state may occur either through an efficient intersystem crossing to the T_1 state or by an ESIPT followed by internal conversion to the S_0 state. An argument for the ESIPT is the observation of the dependence of the blue fluorescence intensity on the nature of the solvent shell.

A relative measure for the interactions between carminic acid and DNA was achieved by performing fluorescence titration measurements. Carminic acid in BPES at the total concentration of c_T = 6 µM was excited at 320 nm. The total fluorescence spectrum between 360 and 800 nm was recorded in the magic-angle polarization configuration. The relative fluorescence intensities (I) were determined by integrating the fluorescence spectra. The fluorescence titrations were performed by detecting the fluorescence spectrum of carminic acid in dependence on the DNA concentration c_{DNA} (M in nucleotide) between 1 nM and 1 mM. Under the simplified approximation that at maximum one carminic acid molecule may bind to one DNA nucleotide, only, the fluorescence titration data may be described by the equation:

$$c_B = \frac{c_T \cdot c_{DNA}}{K_B^{-1} + c_{DNA}},$$

with K_B representing the intrinsic binding constant. The fluorescence intensities of carminic acid in the absence of DNA (I_0), in the course of the titration with DNA (I) and at high DNA concentrations, *i.e.* the plateau value (I_∞), are used to calculate the concentration of free carminic acid:

$$c_F = \frac{c_T (I - I_\infty)}{I_0 - I_\infty}.$$

This relationship allows for the determination of the concentration of bound carminic acid with $c_B = c_T - c_f$. Fig. 5 shows the fluorescence titration curve depicted as the concentration of

bound carminic acid, c_B, versus the DNA concentration, c_{DNA}. An intrinsic binding constant, $K_B = 5.0\times10^5$ (M nucleotide)$^{-1}$ provided the best fit (thick solid line) to the experimental data (dots). The uncertainty in this parameter is about 10 %. This large binding constant agrees very well with that reported for the doxorubicin-calf thymus DNA complex with $K_B = 1.5\times10^5$ (M bp)$^{-1}$ [24] and that of the daunomycin-DNA complexes with $K_B = 7\times10^5$ (M bp)$^{-1}$ [1]. Binding constants of that order of magnitude are typical for strong intercalative bindings of chromophores to the DNA base pairs [24,1].

B. Femtosecond time-resolved spectroscopy

The excited-state decay dynamics of carminic acid in BPES were investigated utilizing fs-resolved transient absorption spectroscopy. Fig.6 represents the temporal evolution of the transient absorption spectra between 0 and 100 ps which is depicted as a 3-D plot. The rather complicated band structure of the spectra obviously originates from a superposition of photobleaching of the ground-state population densities (absorption > 0) and transient absorption of the excited states (absorption < 0). In order to analyze the time evolution of the involved spectral components, we have decomposed each spectrum into 8 Gaussian functions, where photobleaching was accounted for by a positive amplitude and transient absorption by a negative amplitude. The Gaussian fits of the transient absorption spectra for delay times τ from 0 ps to 100 ps in steps of 5 ps were calculated by keeping constant the peak positions and the widths of the Gaussian functions, whereas the amplitudes of the Gaussians were varied until the best fit was obtained. The temporal evolution of each amplitude, as being a measure for the relative absorption of the respective spectral component, could be described by a mono-exponential function. The exponential fits yielded four different time constants for the 8 spectral components, which are $\tau_{ta} = 15\pm0.5$ ps, 20 ± 0.8 ps, 33 ± 1.2 ps and 46 ± 1.4 ps. This result agrees well with the observation of four different species of carminic acid (*i.e.*

CAH, CAH T3, CA^-, CA^- T3) in the stationary absorption spectrum. Hence each set of components with equal time constants constitutes a transient absorption spectrum of one species of carminic acid, respectively. Fig.7 exemplarily displays the transient absorption spectrum (thin solid line) recorded at the delay time τ= 1 ps. The Gaussian fit (thick short dashed line) results from the superposition of 8 Gaussian functions that are assigned to the four different time constants (thick solid, dashed, dashed dotted and dashed double dotted lines).

Complementary informations of excited-state decay behavior were obtained from fluorescence up-conversion experiments. The rather small fluorescence quantum yield of carminic acid limits the detection of the up-converted fluorescence emission to the wavenumber range of 13800 – 17200 cm^{-1}, and thereupon to the observation of two fluorescence bands, only, one peaked at 14910 cm^{-1} and assigned CA^- T3 and the other one at 16490 cm^{-1} ascribed to CAH T3 (*see* Fig.8). Fig. 9 shows the the 3D-plot of carminic acid in BPES at a concentration of 0.6 mM. Addition of DNA at a surplus concentration of 3.9 mM (in nucleotide) does not change the spectral features but distorts a little their time evolution (*see* Fig.10). To achieve indepth insight into the fluorescence decay dynamics and in particular, to explore the influence of the intercalative interaction with DNA, the up-conversion decay curves detected at 14910 cm^{-1} and 16490 cm^{-1}, respectively, both, in the parallel-polarization and perpendicular-polarization geometry, were recorded (see Figs.11 – 14). Figs. 11 and 12 depict the up-conversion decays of carminic acid in BPES, whereas those of carminic acid in BPES in the presence of DNA are shown in Figs. 13 and 14.

The decay curves were evaluated by a merged nonlinear fitting/deconvolution process directly on the parallel (I_{par}) and perpendicular (I_{perp}) signals, using the model functions

$$i_{par}(t) = (1 + 2r(t))\, f(t)$$

$$i_{perp}(t) = (1 - r(t))\, f(t)$$

These were convoluted by the Gaussian model function, $I(t) \propto i(t) \otimes G(t)$. In the fitting we used $f(t) = const. + a \cdot exp(-t/\tau_1) + (1-a) \cdot b \cdot exp(-t/\tau_2)$ and $r(t) = r0 \cdot exp(-t/\tau_{rot})$, where τ_{rot} = 196 ps [13]. I_{par} and I_{perp} represent the fluorescence intensity that was detected in the parallel and perpendicular polarization geometry, respectively. Table 2 contains the amplitudes, a and b, the time constants, τ_1 and τ_2, as well as the anisotropy parameter r(0), which were obtained from the best fit. The short time constants τ_1 were ascribed to a fast structural relaxation process, whereas the long time constants τ_2, with 33±0.7 ps and 47±1 ps, coincide with two excited-state lifetimes obtained from the Gaussian analysis of the transient absorption spectroscopic data. These lifetimes were assigned to the excited-states of the carminic acid tautomers CA^- T3 and CAH T3, respectively. As obvious from figs. 13 and 14, the presence of DNA is associated with a significant prolongation of these lifetimes: τ_2 changes from 33 ps to 48 ps for CA^- T3, whereas CAH T3 exhibits an increase from 47 ps to 61 ps. In addition, the anisotropy parameter r(0) becomes significantly larger under the influence of DNA. The latter effect confirms for another time the efficient couplings of carminic acid to DNA. Moreover, the prolongation of the lifetimes arises from the aprotic rigid environment of the carminic acid incorporated between the DNA base pairs which presumably decelerates the nonradiative processes that are the internal conversion and the intersystem crossing of carminic acid. Reverse ESIPT processes to the excited state of the corresponding normal form are very unlikely to take place because of its higher excited-state energy. Since fluorescence up-conversion were generated using a pump pulse at 400 nm, there are two excitation pathways to populate the excited-states of the tautomers, CAH T3 and CA^- T3. One pathway is direct photoexcitation of the tautomers in their ground state and the other one occurs via ESIPT from the excited state of the corresponding normal form (CAH and CA^-). The rise of all fluorescence up-conversion decay curves (*see* Figs.11 - 14) takes place within the instrumental response time (270 fs). This may be explained by an ultrafast

ESIPT with a proton-transfer time constant smaller than 270 fs. Just as probable is that no ESIPT takes place and the observed fluorescence originates from the directly photoexcited tautomers. On the other hand, the solvent dependence of the blue and orange fluorescence intensities (*see* Figs.1 and 2) unambiguously indicates to the occurrence of ESIPT. This is consistent with the results obtained from fs transient absorption spectroscopy studies of 1,8-dihydroxy-anthraquinone by Neuwahl and coworkers [23]. The authors reported of the observation of a practically instantaneous ESIPT with a proton-transfer time constant much smaller 100 fs.

4. Conclusion

In a buffer solution at pH= 7 carminic acid was found to occur as non dissociated acid (CAH) and as its deprotonated anion (CA^-), both, at nearly the same concentration. The Gaussian analysis of the uv/vis absorption spectrum (*see* Fig.3) gave indication to four species of carminic acid coexisting in the ground state. On the basis of semiempirical molecular geometry computations these four species were assigned to the normal forms of CAH and CA^- and to their corresponding tautomers, CAH T3 and CA^- T3. The existence of four ground-state species was confirmed by femtosecond transient absorption spectroscopy experiments. The Gaussian analysis of the spectroscopic data yielded four different excited-state lifetimes: 15 ps, 20 ps, 33 ps and 46 ps. The solvent dependence of the blue and orange fluorescence intensity is taken as evidence of ESIPT. Carminic acid dissolved in the aprotic solvent DMSO does not exhibit blue fluorescence. On the other hand, in protic environment (BPES) the orange to blue fluorescence intensity ratio is about 2:1, whereas the presence of DNA alters this ratio to 0.8:1. This implies that ESIPT takes instantaneously place in an aprotic medium that is also partially achieved for carminic acid by intercalating between the base pairs of DNA. Fluorescence up-conversion experiments conducted on carminic acid in BPES led to two lifetimes, 33 ps and 47 ps, that were assigned to the tautomers CA^- T3 and

CAH T3 of non dissociated and deprotonated carminic acid, respectively. Since the rise time of fluorescence up-conversion transients corresponds to the instrumental response time constant of 270 fs, only ultrafast ESIPT with a proton-transfer time constant smaller than 100 fs may be involved in the excitation of the tautomers. In the presence of DNA the observed lifetimes increase from 33 ps to 48 ps for CA^- T3 and from 47 ps to 61 ps for CAH T3. Their prolongation in the presence of DNA additionally evidences the formation of intercalation complexes between DNA and carminic acid. The rigid aprotic environment between the DNA base pairs are expected to slow down the nonradiative desactivation processes of the electronically excited carminic acid which are internal conversion and intersystem crossing [19].

Acknowledgement

Financial support by the Access to Research Infrastructures activity in the Sixth Framework Programme of the EU (contract RII3-CT-2003-506350, Laserlab Europe) for conducting the research is gratefully acknowledged.

References

[1] J. B. Chaires, N. Dattagupta and D.M. Crothers, Biochemistry 24 (1985) 260

[2] X. Qu, J. O. Trent, I. Fokt, W. Priebe and J. B. Chaires Proc. Nat. Acad. Sci. USA **97** (2000) 12032

[3] W.A. Remers, "The chemistry of antitumor antibiotics", Wiley, New York, 1979, Vol 1.

[4] A. H.-J. Wang, G. Ughetto, G. J. Quigley and A. Rich, Biochemistry **26** (1987) 1152.

[5] A. Andreoni, A. Colasanti, A. Kisslinger, M. Mastrocinque, G. Portella, P. Riccio and G. Roberti, Photochem. Photobiolog. **57** (1993) 851.

[6] D. Zhong, S. K. Pal, Ch. Wan and A. H. Zewail, PNAS **98** (2001) 11873.

[7] X. Qu, C. Wan, H.-C. Becker, D. Zhong and A. H. Zewail, PNAS **98** (2001) 1421.

[8] C. Wan, T. Xia, H.-C. Becker, and A. H. Zewail, Chem. Phys. Lett. **412** (2005) 158.

[9] J. B. Chaires, N. Daatagupta and D. M. Crothers, Biochemistry **21** (1982) 3933.

[10] J. B. Chaires, W. Priebe, D. E. Graves and T. G. Burke, J. Am. Chem. Soc. **115** (1993) 5360.

[11] C. A. Frederick, L. D. Williams, G. Ughetto, G. A. van der Marel, J. H. van Boom, A. Rich and A. H.-J. Wang, Biochemistry **29** (1990) 2538.

[12] J. P. Rasimas and G. J. Blanchard, J. Phys. Chem. **98** (1994) 12949

[13] J. P. Rasimas and G. J. Blanchard, J. Phys. Chem. **99** (1995) 11333

[14] J. P. Rasimas, K. A. Berglund, and G. J. Blanchard, J. Phys. Chem. **100** (1996) 7220.

[15] R. F. Kubin and A. N. Fletcher, J. Luminescence **27** (1982) 455 – 462.

[16] S. Pommeret, R. Naskrecki, P. van der Meulen, M. Menard, G. Vigneron and T. Gustavsson, Chem. Phys. Lett. **228** (1998) 833.

[17] T. Gustavsson, L. Cassara, V. Gulbinas, G. Gurzadyan, J.-L. Mialocq, S. Pommeret , M. Sorgius and P. van der Meulen, J. Phys. Chem. **A 102** (1998) 4229.

[18] J.E. Ridley and M. Zerner, Theor. Chim. Acta **32** (1973) 111.

[19] T. P. Smith, K. A. Zaklika, K. Thakur, G. C. Walker, K. Tominaga and P. F. Barbara, J. Phys. Chem. **95** (1991) 10465.

[20] G. Smulevich and P. Foggi, J. Chem. Phys. **87** (1987) 5657.

[21] G. Smulevich, P. Foggi, A. Feis and M. P. Marzocchi, J. Chem. Phys. **87** (1987) 5664.

[22] M. P. Marzocchi, A. R. Mantini, M. Casu, and G. Smulevich, J. Chem. Phys. **107** (1998)

[23] F. V. R. Neuwahl, L. Bussoti, R. Righini and G. Buntinx, Phys. Chem. Chem. Phys. **3** (2001) 1227.

[24] J.B. Chaires, W. Triebe, D.E. Graves and T.G. Burke, J. Am. Chem. Soc. **115** (1993) 5360-5364

Figure Captions

Scheme 1. Dissociation reaction of carminic acid (CAH) to its anion (CA^-).

Scheme 2. Molecular structures of the normal form (CAH) and the three tautomers of carminic acid (CAH T1, CAH T2, CAH T3).

Figure 1. Fluorescence spectra of 5 µM carminic acid in BPES (left panel) and in DMSO (right panel); the excitation wavelength was 340 nm.

Figure 2. Normalized fluorescence spectra of 5 µM carminic acid in BPES (dashed line) and of 5 µM carminic acid with 5 µM DNA in BPES (solid line).

Figure 3. Absorption spectra of carminic acid in BPES (left panel) and in DMSO (right panel); the band structure of the spectra (thin solid line) was analyzed by fitting with a superposition of four Gaussian functions (dashed line).

Figure 4. The spectra of the orange fluorescence of 5 µM carminic acid in BPES (left panel) and in DMSO (right panel); the band structure of the spectra (thin solid line) was analyzed by fitting with a superposition of four Gaussian functions (dashed line).

Figure 5. Concentration dependence of bound carminic acid, c_B, on the DNA concentration; the experimental data (dots) were obtained from fluorescence titration of 6 µM carminic acid with DNA in BPES and were fitted (solid line) employing the relationship $c_B = c_T \cdot c_{DNA}/(K_B^{-1} + c_{DNA})$ with $K_B = 5.0 \times 10^5$ (M nucleotide)$^{-1}$.

Figure 6. 3-D plot of the temporal evolution of the transient absorption spectra obtained for carminic acid in BPES.

Figure 7. Transient absorption spectrum (thin solid line) recorded at the delay time $\tau = 1$ ps; The fit (thick short dashed line) arises from the superposition of 8 Gaussian functions

assigned to four different time constants (thick solid, dashed, dashed dotted and dashed double dotted lines).

Figure 8. Fluorescence-up conversion spectrum (dots) fitted by a superposition (thin solid line) of two Gaussians (dashed line).

Figure 9. 3-D plot of the temporal evolution of the fluorescence up-conversion spectra obtained for 0.6 mM carminic acid in BPES.

Figure 10. 3-D plot of the temporal evolution of the fluorescence up-conversion spectra obtained for 0.6 mM carminic acid and 3.9 mM DNA in BPES.

Figure 11. Fluorescence up-conversion decays of 0.6 mM carminic acid in BPES (thin solid line) detected at 14910 cm^{-1} in the parallel-polarization geometry ($I(t)_{par}$) and in the perpendicular-polarization geometry ($I(t)_{perp}$); both fits were obtained using the parameter: a= 0.37, b= 0.91, τ_1= 1.7 ps, τ_2= 33 ps and r(0)= 0.137.

Figure 12. Fluorescence up-conversion decays of 0.6 mM carminic acid in BPES (thin solid line) detected at 16490 cm^{-1} in the parallel-polarization geometry ($I(t)_{par}$) and in the perpendicular-polarization geometry ($I(t)_{perp}$); both fits were obtained using the parameter: a= 0.50, b= 0.92, τ_1= 1.5 ps, τ_2= 47 ps and r(0)= 0.202.

Figure 13. Fluorescence up-conversion decays of 0.6 mM carminic acid and 3.9 mM DNA in BPES (thin solid line) detected at 14910 cm^{-1} in the parallel-polarization geometry ($I(t)_{par}$) and in the perpendicular-polarization geometry ($I(t)_{perp}$); both fits were obtained with the parameter: a= 0.50, 0.97, τ_1= 1.9 ps, τ_2= 48 ps and r(0)= 0.182.

Figure14. Fluorescence up-conversion decays of 0.6 mM carminic acid and 3.9 mM DNA in BPES (thin solid line) detected at 16490 cm^{-1} in the parallel-polarization geometry ($I(t)_{par}$) and in the perpendicular-polarization geometry ($I(t)_{perp}$); both fits were obtained with the parameter: a= 0.50, b= 0.97, τ_1= 1.1 ps, τ_2= 61 ps and r(0)= 0.243.

Tables

Table 1. Calculated values of the total energy (E_T), the binding energy (E_B), the absolute energy (E_{abs}), the wavenumber of the two lowest-energy absorption transitions, *i.e.* the S_0-S_m transition ($\Delta(S_0\text{-}S_m)$) and the S_0-S_n transition ($\Delta(S_0\text{-}S_m)$) transition, and their oscillatory strength (f).

	E_T/kcal/mol	E_B/kcal/mol	E_{abs}/eV	$\Delta(S_0\text{-}S_m)/cm^{-1}$	f	$\Delta(S_0\text{-}S_n)/cm^{-1}$	f
CAH	-185444	-25700	-8041.5	22716	0.269	23492	0.037
CA^-	-184815	-25378	-8014.2	20563	0.071	23496	0.148
CAH T1	-185427	-25693	-8040.7	19351	0.606	21801.1	0.056
CA^- T1	-184851	-25421.3	-8015.8	18281.1	0.632	23061.6	0.031
CAH T2	-185431	-25698.3	-8040.9	18919	0.555	25395	0.070
CA^- T2	-184811	-25579	-8014	19087.7	0.683	25944.7	0.041
CAH T3	-185440	-25707	-8041.3	18900	0.393	28473.5	0.029
CA^- T3	-184820	-25397.7	-8014.4	15491.4	0.414	21758.3	0.051

Table 2. The amplitudes, a and b, the time constants, τ_1 and τ_2, and the anisotropy, r(0), were obtained from the best fit of the fluorescence up-conversion decay curves that are detected at 14910 $cm^{-1}$and 16490 cm^{-1}.

	a	b	τ_1 / ps	τ_2 / ps	r(0)
CA^-T3: 14910 cm^{-1}	0.37	0.91	1.7	33	0.137
CAHT3: 16490 cm^{-1}	0.50	0.92	1.5	47	0.202
CA^-T3+DNA: 14910 cm^{-1}	0.50	0.97	1.9	48	0.182
CAHT3+DNA: 16490 cm^{-1}	0.50	0.97	1.1	61	0.243

Schemes and Figures

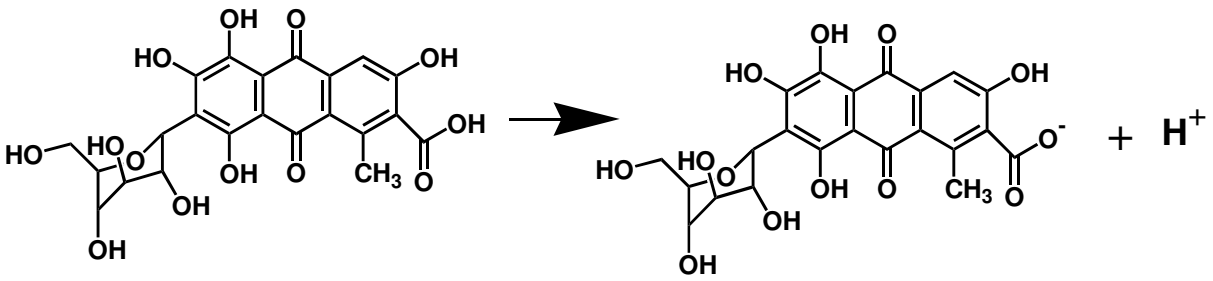

Scheme 1

CAH:

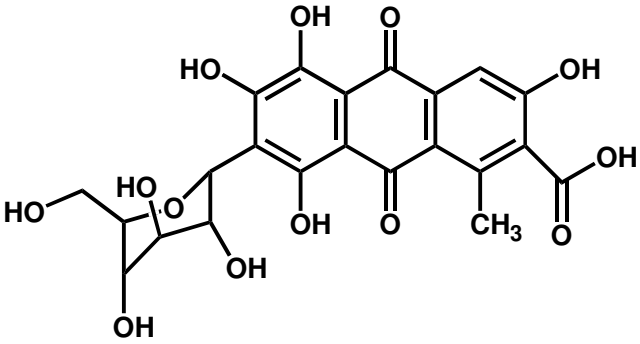

CAH T1:

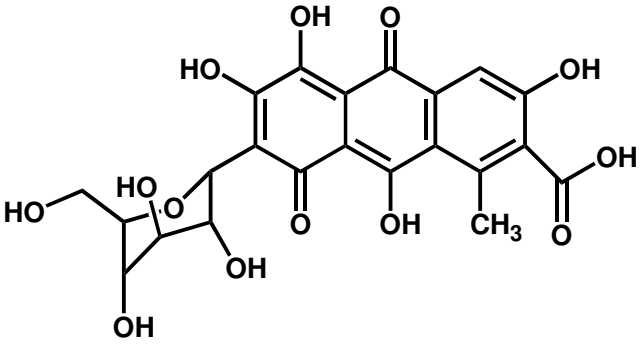

CAH T2:

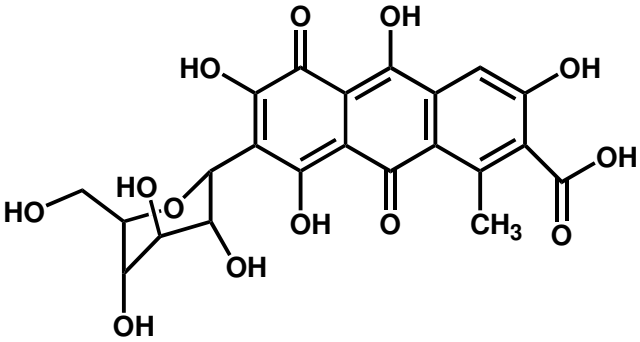

CAH T3:

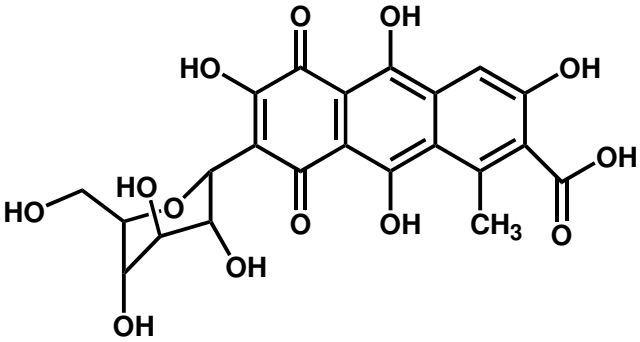

Scheme 2

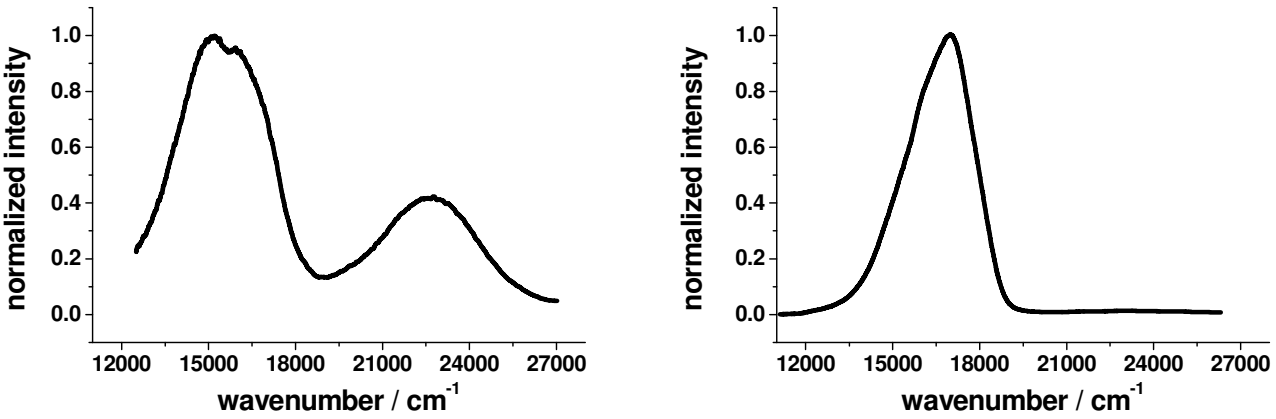
normalized intensity
1.0
0.8
0.6
0.4
0.2
0.0
12000
15000
18000
21000
24000
27000
wavenumber / cm-1
normalized intensity
1.0
0.8
0.6
0.4
0.2
0.0
12000
15000
18000
21000
24000
27000
wavenumber / cm-1

Fig.1

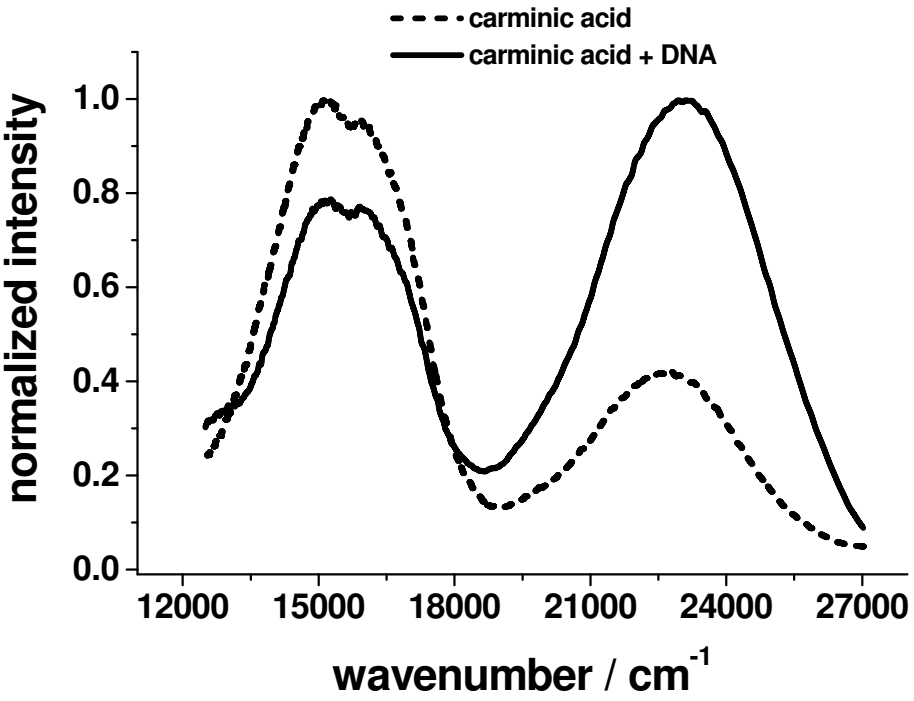
carminic acid
carminic acid + DNA
normalized intensity
1.0
0.8
0.6
0.4
0.2
0.0
12000
15000
18000
21000
24000
27000
wavenumber / cm-1

Fig.2

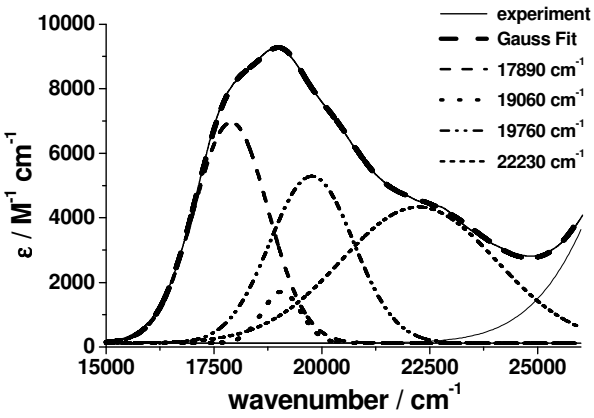
experiment
Gauss Fit
17890 cm-1
19060 cm-1
19760 cm-1
22230 cm-1
ε / M-1 cm-1
wavenumber / cm-1

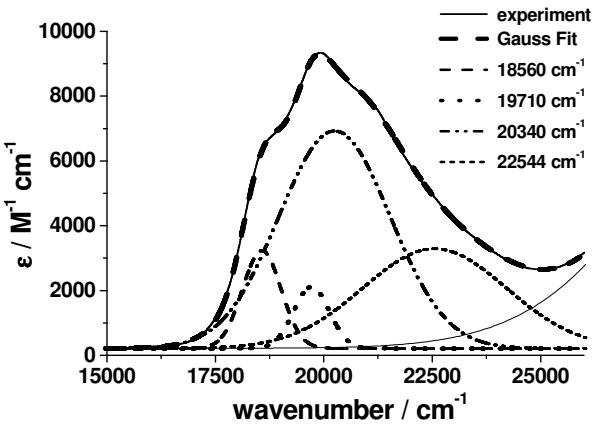
experiment
Gauss Fit
18560 cm-1
19710 cm-1
20340 cm-1
22544 cm-1
ε / M-1 cm-1
wavenumber / cm-1

Fig.3

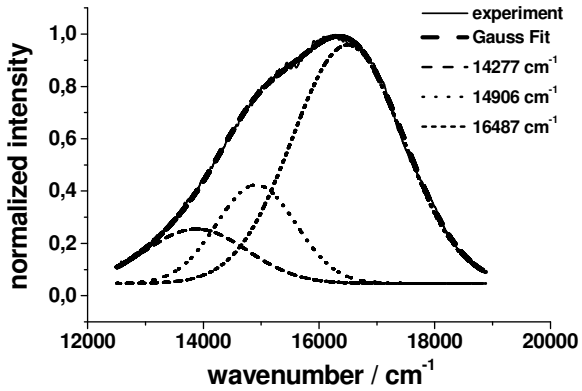
experiment
Gauss Fit
14277 cm-1
14906 cm-1
16487 cm-1
normalized intensity
wavenumber / cm-1

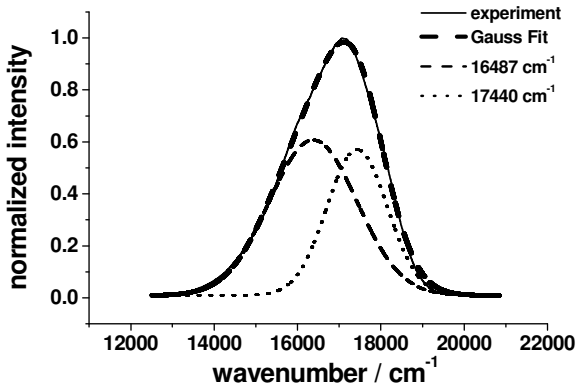
experiment
Gauss Fit
16487 cm-1
17440 cm-1
normalized intensity
wavenumber / cm-1

Fig. 4

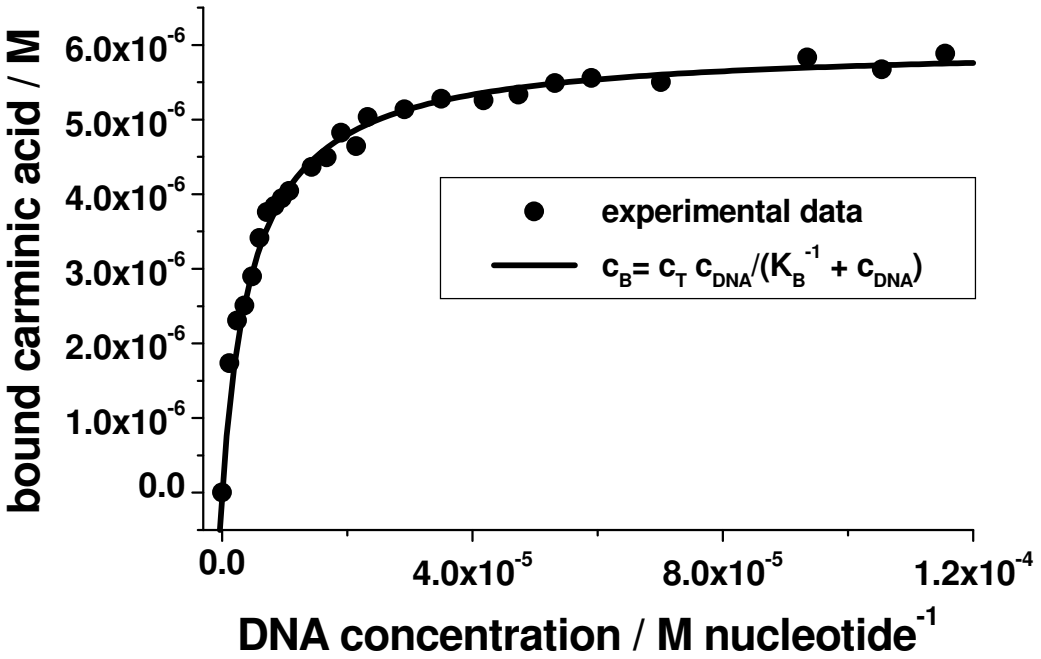
bound carminic acid / M
6.0x10-6
5.0x10-6
4.0x10-6
3.0x10-6
2.0x10-6
1.0x10-6
0.0
experimental data
cB= cT cDNA/(KB-1 + cDNA)
0.0
4.0x10-5
8.0x10-5
1.2x10-4
DNA concentration / M nucleotide-1

Fig. 5

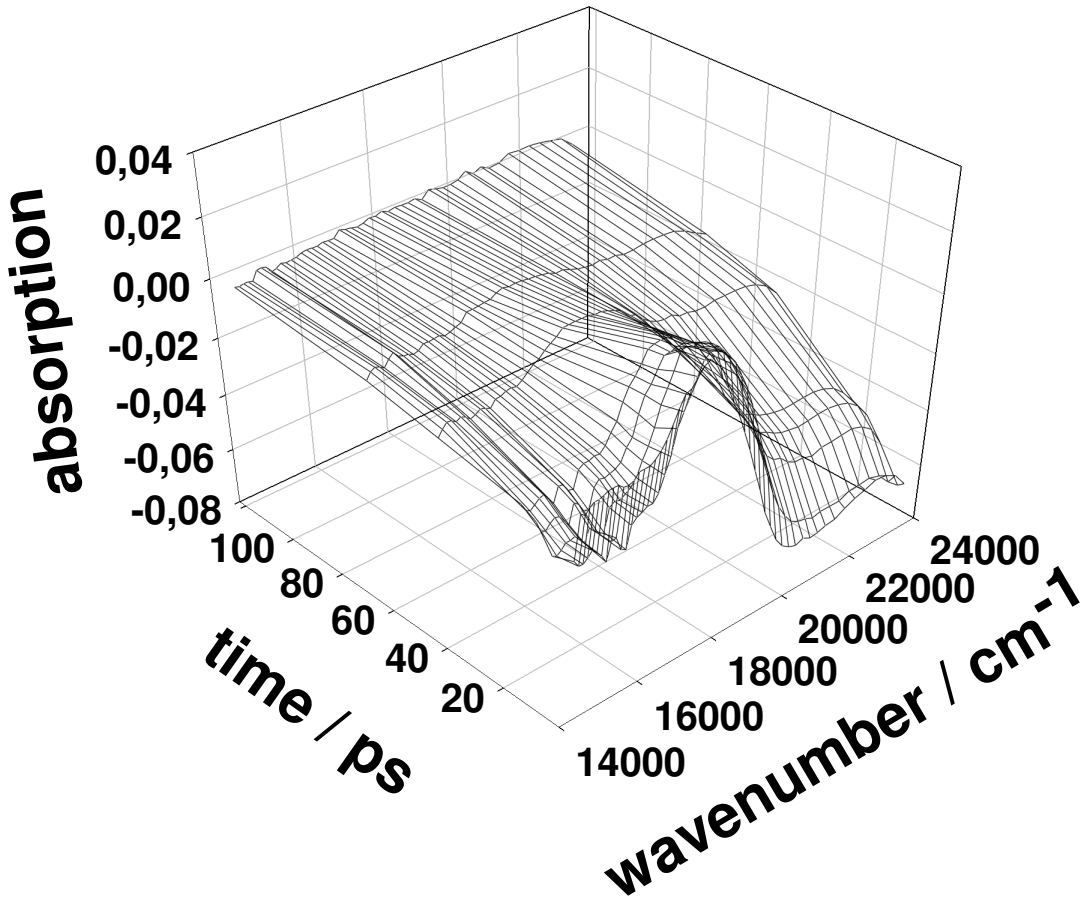
absorption
0,04
0,02
0,00
-0,02
-0,04
-0,06
-0,08
time / ps
100
80
60
40
20
wavenumber / cm-1
24000
22000
20000
18000
16000
14000

Fig.6

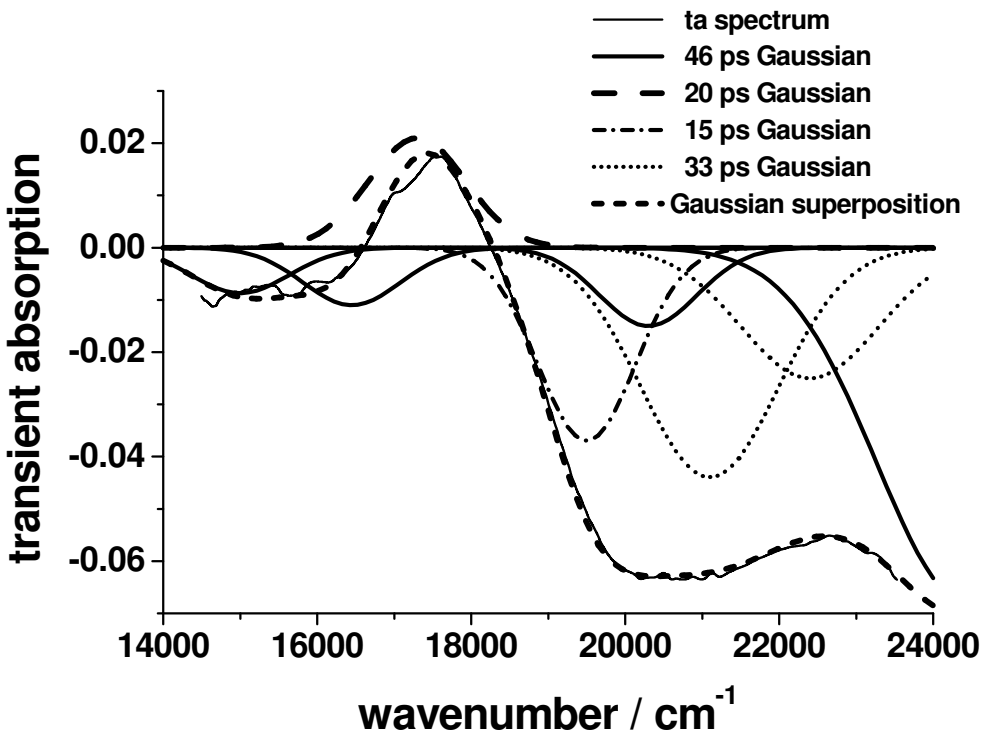
ta spectrum
46 ps Gaussian
20 ps Gaussian
15 ps Gaussian
33 ps Gaussian
Gaussian superposition
transient absorption
0.02
0.00
-0.02
-0.04
-0.06
14000
16000
18000
20000
22000
24000
wavenumber / cm-1

Fig.7

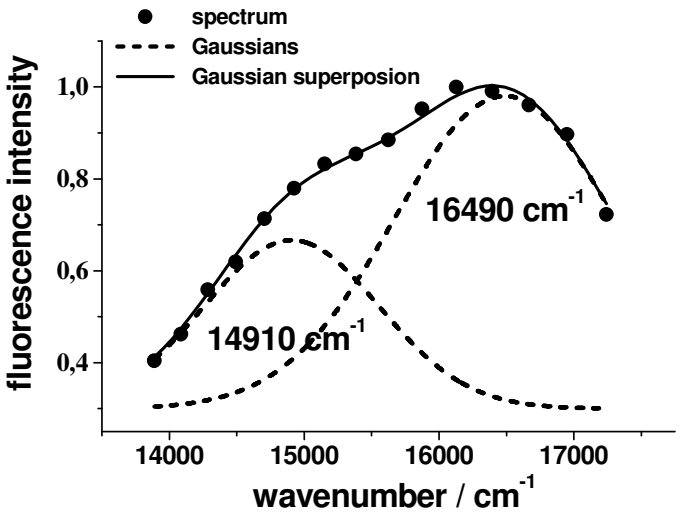
spectrum
Gaussians
Gaussian superposion
fluorescence intensity
1,0
0,8
0,6
0,4
16490 cm-1
14910 cm-1
14000
15000
16000
17000
wavenumber / cm-1

Fig. 8

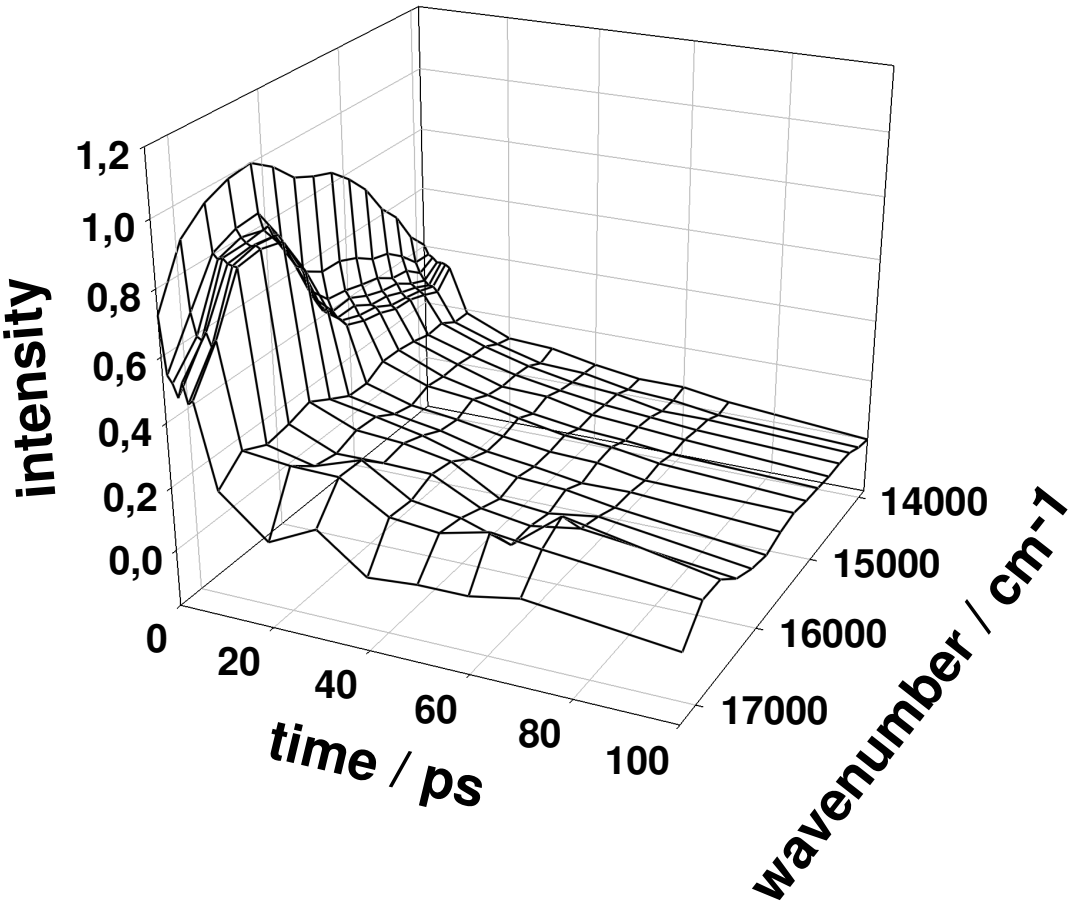
intensity
1,2
1,0
0,8
0,6
0,4
0,2
0,0
0
20
40
60
80
100
time / ps
14000
15000
16000
17000
wavenumber / cm-1

Fig.9

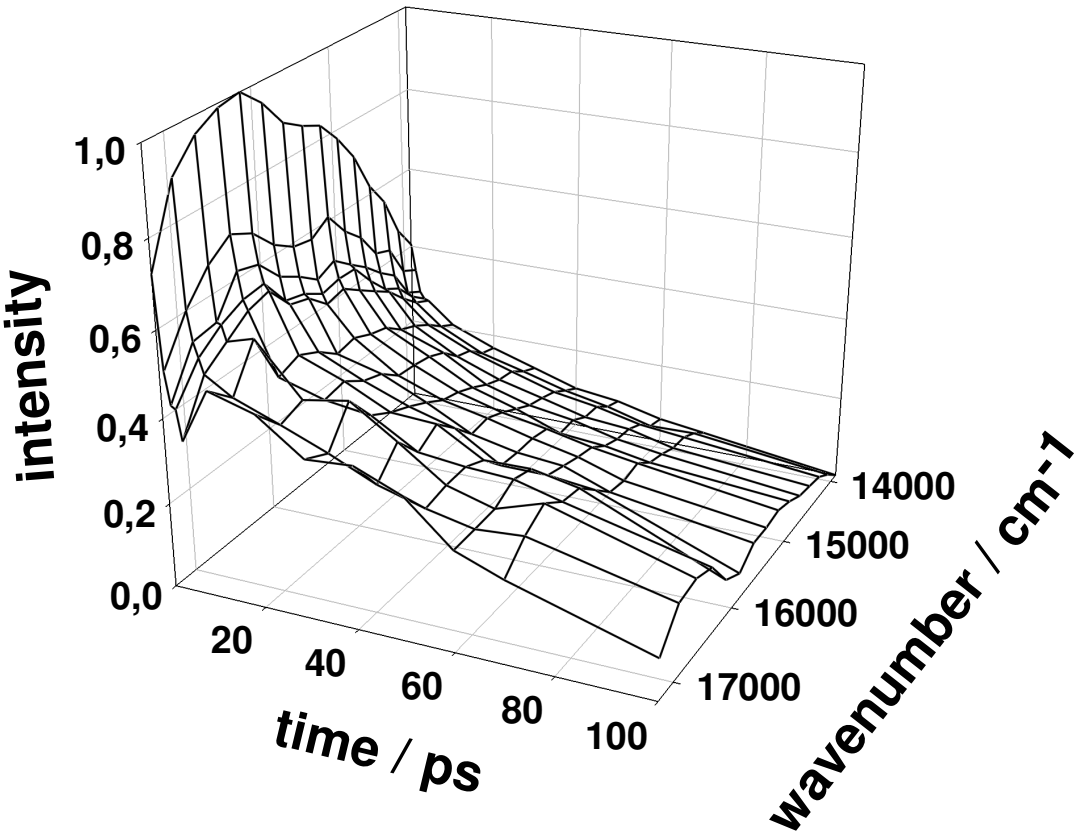
intensity
1,0
0,8
0,6
0,4
0,2
0,0
20
40
60
80
100
time / ps
14000
15000
16000
17000
wavenumber / cm-1

Fig. 10

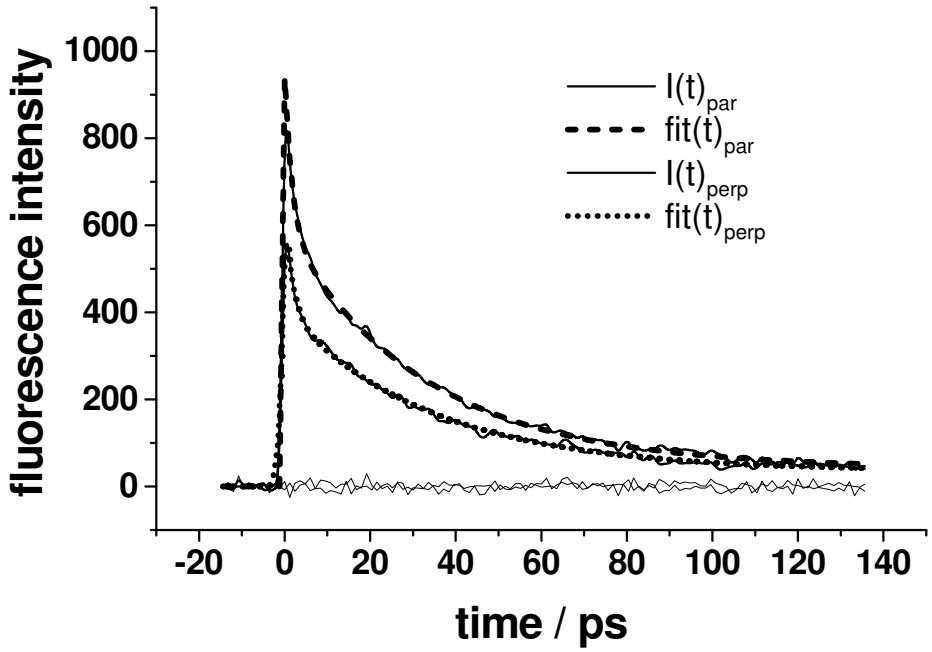
fluorescence intensity
1000
800
600
400
200
0
-20
0
20
40
60
80
100
120
140
time / ps
I(t)par
fit(t)par
I(t)perp
fit(t)perp

Fig. 11

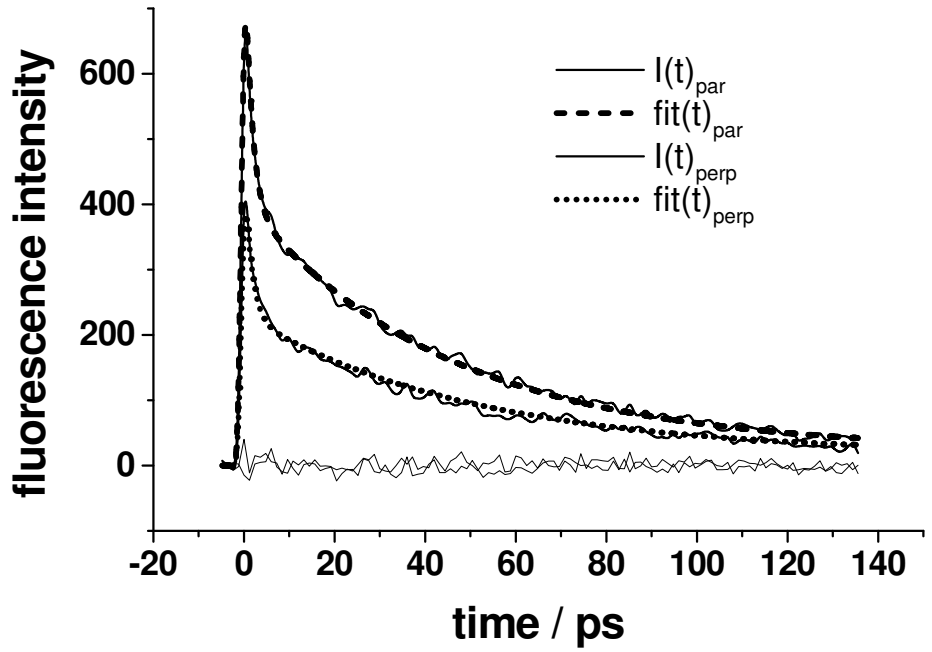
fluorescence intensity
600
400
200
0
-20
0
20
40
60
80
100
120
140
time / ps
I(t)par
fit(t)par
I(t)perp
fit(t)perp

Fig. 12

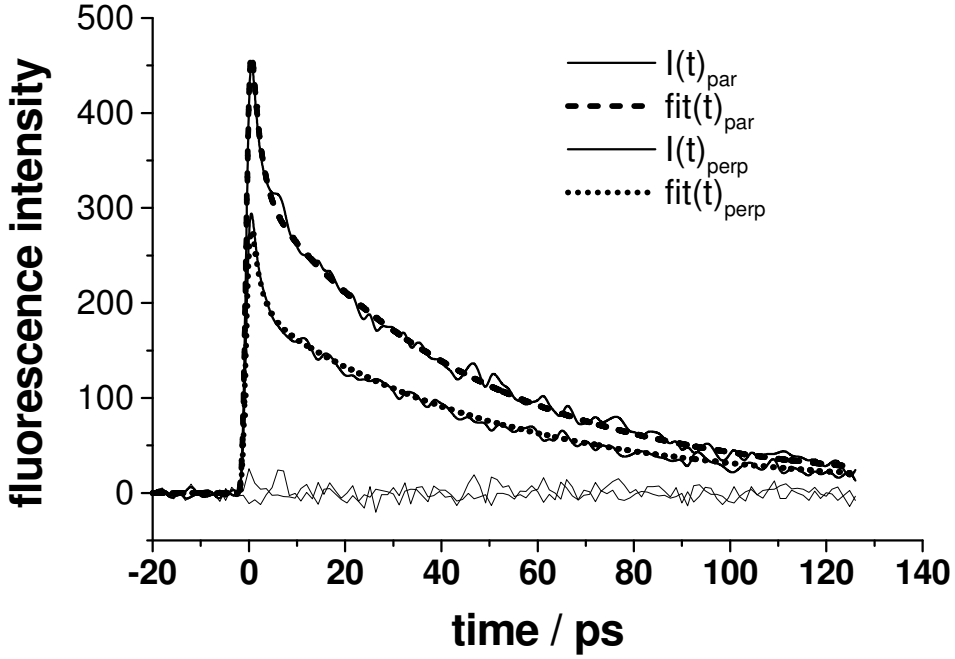
fluorescence intensity
time / ps
I(t)par
fit(t)par
I(t)perp
fit(t)perp
500
400
300
200
100
0
-20
0
20
40
60
80
100
120
140

Fig. 13

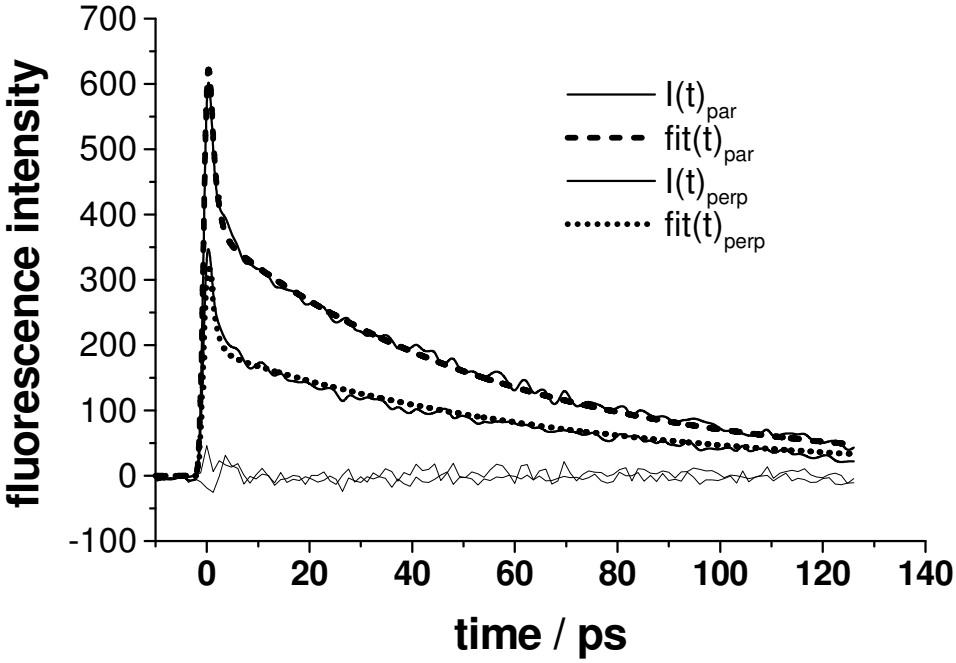
fluorescence intensity
time / ps
I(t)par
fit(t)par
I(t)perp
fit(t)perp
700
600
500
400
300
200
100
0
-100
0
20
40
60
80
100
120
140

Fig. 14